

Research Articles: Systems/Circuits

Early life pain experience changes adult functional pain connectivity in the rat somatosensory and the medial prefrontal cortex

<https://doi.org/10.1523/JNEUROSCI.0416-22.2022>

Cite as: J. Neurosci 2022; 10.1523/JNEUROSCI.0416-22.2022

Received: 1 March 2022

Revised: 19 August 2022

Accepted: 24 August 2022

This Early Release article has been peer-reviewed and accepted, but has not been through the composition and copyediting processes. The final version may differ slightly in style or formatting and will contain links to any extended data.

Alerts: Sign up at www.jneurosci.org/alerts to receive customized email alerts when the fully formatted version of this article is published.

1 **Early life pain experience changes adult functional pain connectivity in the rat somatosensory and**
2 **the medial prefrontal cortex**

3 **Pishan Chang, Lorenzo Fabrizi and Maria Fitzgerald***

4 Department of Neuroscience, Physiology & Pharmacology, Medawar Pain and Somatosensory Labs,
5 University College London, London WC1E 6BT, UK

6 *Correspondence: m.fitzgerald@ucl.ac.uk

7 **Abbreviated Title:** Early life pain and adult cortical connectivity

8 **Number of pages:** 17

9 **Number of figures:** 6

10 **Number of words:-**

- 11 • **Abstract:** 203
- 12 • **Introduction:** 664
- 13 • **Discussion:** 1774

14 **The authors declare that they have no conflict of interest**

15 **Acknowledgments:** Supported by grants from the Biotechnology and Biological Sciences Research
16 Council (MF, PC) (BB/R00823X/1) and the Medical Research Council (LF, MF) (MR/L019248/1).

17

18 **Abstract**

19 Early life pain experience (ELP) alters adult pain behaviour and increases injury induced pain hypersensitivity,
20 but the effect of ELP upon adult functional brain connectivity is not known. We have performed continuous
21 local field potential (LFP) recording in the awake adult male rats to test the effect of ELP upon functional
22 cortical connectivity related to pain behaviour. Somatosensory cortex (S1) and medial prefrontal cortex
23 (mPFC) LFPs evoked by mechanical hindpaw stimulation were recorded simultaneously with pain reflex
24 behaviour for 10 days after adult incision injury. We show that, post adult injury, sensory evoked S1 LFP
25 delta and gamma energy and S1 LFP delta/gamma frequency coupling are significantly increased in ELP rats
26 compared to controls. Adult injury also induces increases in S1-mPFC functional connectivity but this is
27 significantly prolonged in ELP rats, lasting 4 days compared to 1 day in controls. Importantly, the increases in
28 LFP energy and connectivity in ELP rats were directly correlated with increased behavioural pain
29 hypersensitivity. Thus, early life pain (ELP) alters adult brain functional connectivity, both within and
30 between cortical areas involved in sensory and affective dimensions of pain. The results reveal altered brain
31 connectivity as a mechanism underlying the effects of early life pain upon adult pain perception.

32 **Keywords:** cortical pain networks, infant pain, experience dependence, brain development, pain
33 development, early life adversity, nociception, nociceptive development.

34 **Significance Statement**

35 Pain and stress in early life has a lasting impact upon pain behaviour and may increase vulnerability to
36 chronic pain in adults. Here we record pain-related cortical activity and simultaneous pain behaviour in
37 awake adult male rats previously exposed to pain in early life. We show that functional connectivity within
38 and between the somatosensory cortex and the medial prefrontal cortex is increased in these rats and that
39 these increases are correlated with their behavioural pain hypersensitivity. The results reveal that early life
40 pain alters adult brain connectivity, which may explain the impact of childhood pain upon adult chronic pain
41 vulnerability.

42 **Introduction**

43 Exposure to pain and injury in early life pain (ELP) is associated with altered pain behaviour in adults.
44 Evidence from both human and animal studies shows that repeated painful procedures or surgical incision
45 during a critical period of early postnatal development has significant long-term effects on pain processing
46 (Walker et al., 2009b, 2009a; Beggs et al., 2012b; Schwaller and Fitzgerald, 2014; van den Hoogen et al.,
47 2018). The mechanisms underlying the effects of ELP involve changes in peripheral cutaneous innervation
48 (Reynolds and Fitzgerald, 1995; De Lima et al., 1999; Beggs et al., 2012a; Boada et al., 2012), peripheral
49 afferent sensitization (Walker et al., 2016; Liu et al., 2017; Dourson et al., 2021), spinal cord nociceptive
50 circuitry (Torsney and Fitzgerald, 2003; Li and Baccei, 2019), early life spinal microglial activation (Moriarty
51 et al., 2019) and altered descending brain stem pain control (Walker et al., 2015). There is also evidence
52 from human studies of structural changes in the thalamus and cortex (Duerden et al., 2018) and functional
53 changes in descending pain control from supraspinal sites (Walker et al., 2018). The importance of this
54 extends into a wider area of the long-term consequences of early life stress and pain which, by inducing
55 long-term alterations in brain function and behaviour may lead to higher susceptibility to chronic pain
56 (Jones et al., 2009; Denk et al., 2014; Ririe et al., 2021; Melchior et al., 2022). However, as yet, there is no
57 evidence that ELP has any effect upon adult cortical pain networks or upon functional connectivity between
58 the key cortical regions involved in the sensory and emotional dimensions of pain.

59 A wide network of brain areas is involved in acute pain processing, including primary (S1) and secondary (S2)
60 somatosensory cortices, the medial prefrontal cortex (mPFC), insula, thalamus, and prefrontal areas
61 (Apkarian et al., 2005; Duerden and Albanese, 2013; Tan and Kuner, 2021). To address whether ELP impacts

62 upon cortical function from the sensory-discriminative and emotional/cognitive perspectives, the S1 and
63 mPFC are attractive targets (Tan and Kuner, 2021). S1 is a functionally defined part of the somatosensory
64 and nociceptive system and processes sensory nociceptive information about pain from an early age in both
65 rodents and humans (Chang et al., 2016, 2020b; Jones et al., 2022). S1 encodes nociceptive intensity and
66 perceived pain intensity (Mancini et al., 2012) and gamma-band oscillations in this area correlate with
67 subjective pain perception (Ong et al., 2019). While mPFC is critically involved in numerous cognitive
68 functions (Euston et al., 2012; Chang et al., 2020a) and emotion behaviour (Cao et al., 2018; Huang et al.,
69 2020), this area also plays an important role in the emotional and affective aspects of pain, and could
70 modulate pain sensation by controlling the flow of afferent sensory stimuli into the dorsal horn through
71 descending control pathways (Zhang et al., 2015; Huang et al., 2020). Here we hypothesise that ELP alters
72 pain related connectivity in the adult S1 and mPFC and that this is associated with increases in adult pain
73 related behaviour.

74 In this study, we used a well-established model of injury and postoperative pain: hind-paw plantar incision of
75 skin and underlying muscle (Brennan et al., 1996; Beggs et al., 2012b) to examine the impact of ELP upon
76 pain behaviour and associated neural activity in S1 and mPFC. We recorded local field potentials (LFPs) in S1
77 and mPFC in awake, freely moving adult rats and analysed the oscillatory energy within those sensory
78 evoked LFPs and the functional connectivity within and between these areas. Acute pain is associated with
79 defined changes in cortical oscillations (Tan et al., 2021). In humans, gamma-band oscillations in S1
80 correlate with subjective pain perception (Heid et al., 2020; Yue et al., 2020a) and are strengthened in
81 rodent S1 cortex during nociception and inflammatory pain in association with behavioural nociceptive
82 hypersensitivity (Tan et al., 2019). We also analyse phase-amplitude coupling and coherence of neuronal
83 oscillations as putative mechanisms of regional and inter-areal communication (Buzsaki, 2004; Peng and
84 Tang, 2016). Together, our results provide new insights into how early life pain (ELP) alters adult cortical
85 function underlying sensory and emotional dimensions of pain behaviour.

86 **Materials and Methods**

87 **Experimental animals:** All experiments were performed in accordance with the United Kingdom Animal
88 (Scientific Procedures) Act 1986. Reporting is based on the ARRIVE Guidelines for Reporting Animal Research
89 developed by the National Centre for Replacement, Refinement and Reduction of Animals in Research,
90 London, United Kingdom. Male Sprague-Dawley rat pups were obtained from the Biological Services Unit,
91 University College London. Rats were housed in cages of five age-matched animals (>P21) or with the dam
92 and littermates (P) 3 to 21 under controlled environmental conditions (24–25°C; 50–60% humidity; 12 h
93 light/dark cycle) with free access to food and water. In the case of rat pups, handling and maternal
94 separation were kept to a minimum. All animals were exposed to the same standard caging, handling and
95 diet throughout development. The different experimental groups are represented in Figure 1A and protocol
96 for probing the impact of nociceptive inputs in the early life on central pain processing and adult pain
97 sensitivity is summarized in Figure 1B

98 **Plantar hind-paw incision:** Male rat pups on postnatal Day 3 were anaesthetized and plantar hindpaw
99 incision performed. Under general anesthesia with 2% isoflurane in 100% oxygen (flow rate, 1–1.5 L/min), a
100 midline longitudinal incision was made through the skin and fascia extending from the midpoint of the heel
101 to the proximal border of the first footpad and the underlying plantar muscle elevated and incised. The same
102 relative length of incision was performed in adult animals as previously described (Brennan et al., 1996;
103 Walker et al., 2009b). Skin edges were closed with 5–0 nylon suture (Ethicon). The whole procedure took 3–5
104 min. After plantar hindpaw incision, rats were placed in a recovery chamber and allowed to recover from the
105 general anesthesia before returning to their home cage.

106 Four experimental groups were used: **II**: neonatal incision on postnatal day 3 and repeat incision 2 months
107 later in adulthood. **NI**: littermate control with equivalent anaesthesia, handling and maternal separation on
108 post-natal day 3 and having incision in adulthood. Animals having neonatal incision and follow-up in
109 adulthood (**IN**) and age-matched non-incised litter mates from the same colony (**NN**) were pooled data and
110 used as control group (**Con**), due to that there is no significant different between the two groups (Figure 1A)

111 **Pain hypersensitivity testing:** To test behavioural pain hypersensitivity following hind-paw incision, an
112 electronic von Frey unit (EVF4, Bioseb) was used to measure hindpaw mechanical flexion withdrawal
113 thresholds (Ferrier et al., 2015, 2016). Following habituation for 30 min on an elevated mesh platform, a
114 mechanical stimulus was applied to the plantar surface of the hindpaw adjacent to the distal half of the
115 incision. The von Frey (eVF) apparatus, which has a measurement range of 0-500 g with 0.1 g resolution,
116 consists of a plastic tip fitted in a hand-held force transducer, which was applied to the rat hindpaw from
117 below with force (g) gradually increased until paw withdrawal. The force that induced paw withdrawal was
118 digitized and recorded automatically by the unit and used as the threshold for mechanical nociception. For
119 each recording session, the eVF was applied 3-5 times at ~50 sec intervals. Simultaneous recording from
120 both S1 and mPFC accompanied testing of eVF withdrawal thresholds (Figure 1 C, D).

121 **Surgical Preparation and Transmitter Implantation for Long-term Recording:** Rats were anaesthetised with
122 2.5-3 % isoflurane (Abbot, AbbVie Ltd., Maidenhead, UK) in 100% oxygen (flow rate of 1-1.5 litre/min) via gas
123 anaesthesia mask (Model 906, David Kopf Instruments) from a recently calibrated vaporizer (Harvard
124 Apparatus, Cambridge, MA). Body temperature was maintained with a heat blanket during surgery. A
125 transmitter (A3028D-DDA, Open Source Instruments, Brandeis, Boston, USA)(Chang et al., 2011) was
126 implanted subcutaneously with the depth recording electrodes (J-electrode (wire 125- μ m dia 316SS 10kOhm
127 impedance), a Teflon-insulated stainless steel electrode, Open Source Instruments, Brandeis, Boston, USA)
128 positioned in mPFC (3.2 mm anterior, 0.5 mm lateral, 4 mm ventral) and primary somatosensory hindpaw
129 cortex (1 mm posterior, 2.5 mm lateral, 2 mm ventral) (Paxinos et al., 2013; Chang et al., 2016). The
130 reference electrode was implanted over the cerebellum posterior to lambda. The whole assembly was held
131 in place with dental cement (Simplex Rapid, Acrylic Denture Polymer, UK). A subcutaneous injection of
132 bupivacaine and metacam was provided for post-surgical pain management. At the end of surgery,
133 enrofloxacin (5mg/kg, Baytril, Bayer health care) and pre-warm saline (0.5-1 ml) were administered
134 subcutaneously. The animals were placed in a temperature controlled (25°C) recovery chamber until
135 ambulatory and closely monitored at least 1-2 hours before returning to their home cage to allow recovery
136 for at least 14 days after surgery.

137 The transmitter, which has no adverse effects (Chang et al., 2016), was implanted for data recordings. During
138 all recording sessions, continuous LFP recordings were recorded (bandpass filter: 0.2 Hz to 160 Hz, 512Hz
139 sampling rate with 16 bit resolution) using LWDQA Software (Open Source Instruments, Brandeis, Boston,
140 USA). Animals were carefully monitored daily and were euthanized at the end of experiment with carbon
141 dioxide (CO₂). The brain was removed and immediately immersed in 4% paraformaldehyde for >24 hours
142 before being transferred to 30% sucrose post-fixation solution. Brain sections (40- μ m thick thickness) were
143 cut using a microtome (Leica SM2000R, Leica Microsystems (UK) Ltd., United Kingdom) and stained with
144 Cresyl violet to allow histological location of the electrode track. This procedure allowed us to verify
145 recording electrode locations, and LFP data were only included in the study if electrode tips were located in
146 mPFC and S1 (Figure 1D).

147 **Analysis of electrophysiology data:** Data analysis was performed with Brainstorm (Tadel et al., 2011), which
148 is free and open source for electrophysiology data visualization and processing through a simple and
149 intuitive graphical user interface (GUI) (<http://neuroimage.usc.edu/brainstorm>) and custom Matlab scripts
150 (The Mathworks Inc.MA, USA).

151 **Evoked LFP data processing: LFP Pre-processing:** For our initial analyses, continuous LFP recordings from
152 each region were segmented into 10s epochs that lasted from 5s before to 5s after the peak of evoked LFP.
153 Each epoch was visually inspected for artefacts prior to further analysis. Any epochs that, upon visual
154 inspection, exhibited electrode artifacts (ie, abrupt vertical transients that do not modify the background
155 activity) were excluded from subsequent analysis. **Time-frequency Analysis:** Activity changes in LFP in
156 different frequency bands were calculated using the Hilbert transform (Le Van Quyen et al., 2001; Bruns,
157 2004; Tadel et al., 2011). Each epoch was filtered in various frequency bands with bandpass filters for delta
158 (2–4 Hz), theta (4–8 Hz), alpha (8–12 Hz), beta (12–30 Hz), and gamma (30–90 Hz) band. The magnitude
159 ($\mu\text{V}/\sqrt{\text{Hz}}$) of the Hilbert transform of a narrow-band signal is a measure of the envelope of this signal,
160 and therefore gives an indication of the activity in this frequency band. The energy magnitude data were
161 then averaged across repetitions within each animal. Stimulus-induced changes in energy magnitude for
162 each animal were then calculated by normalized to mean of baseline (-4 to -1s).

163 **Time-resolved Phase-amplitude Coupling Analysis:** This approach measures cross-frequency coupling
164 between bursts of high-frequency oscillations and the phase of lower frequency rhythms, over a time-
165 window, which slides along the electrophysiological data (Samiee and Baillet, 2017). mPFC and S1 time-
166 courses were examined for changes in phase of slow oscillation at delta band (2-4 Hz) coupled to the
167 amplitude of a faster rhythm at gamma (30-90 Hz) band. Phase and amplitude information were obtained
168 via the Hilbert transform. The coupling between phase and amplitude was then quantified and Modulation
169 Index values were calculated. To avoid edge artefacts, which can result in spurious phase-amplitude coupling
170 (PAC) (Kramer et al., 2008), the first 2 s and last 2 s of each trial was used as buffer. These were then
171 averaged across repetitions within each animal. Stimulus-induced Phase-Amplitude Coupling for each animal
172 were then calculated by normalized to mean of baseline (-2.5 to -1 s). **Time-resolved Phase locking**
173 **Analysis:** To evaluate the functional connectivity between mPFC and S1, we estimated phase-locking value
174 between the LFPs simultaneously recorded at the two areas in different frequency bands (Lachaux et al.,
175 1999). To do this we (i) band-pass filtered the LFPs at S1 and mPFC in the delta (2–4 Hz), theta (4–8 Hz),
176 alpha (8–12 Hz), beta (12–30 Hz), and gamma (30–90 Hz) frequency bands; (ii) applied Hilbert transform to
177 the band-passed signals; (iii) calculate the instantaneous phase-locking value between mPFC and S1. PLVs
178 were then averaged across repetitions within each animal. Stimulus-induced magnitude changes in LFP
179 energy for each animal were then calculated by normalized to mean of baseline (-4 to -1s)

180 **Quantification and Statistical Analysis:** Statistical analysis was performed using GraphPad Prism 6
181 (GraphPad Software), SPSS (Statistical Product and Service Solutions, IBM). All data are presented as mean \pm
182 SEM. Comparisons of means were performed using one way ANOVA with Tukey post hoc test if the data
183 were normally distributed; Kruskal-Wallis test with post hoc Dunn's multiple comparisons test if the data
184 were not normally distributed (with the Shapiro-Wilk test used to assess normality of the data distributions).
185 Generalized linear model (GLM) Type III tests followed by Bonferroni post hoc tests were used for analysis of
186 repeated-measures behaviour data. Differences were considered statistically significant at $p < 0.05$.
187 Estimation statistics (open source estimation program available on <https://www.estimationstats.com>) (Ho et
188 al., 2019) were used to compute the change of electrophysiological data in mPFC/S1 in response to eVF
189 stimulation with days following injury (D0, D4, and D10), compared to pre-injury activity. Mean differences
190 are shown using Cumming estimation plots, with each graphed as a bootstrap sampling distribution (5000
191 bootstrap samples). The p value(s) reported are the likelihood(s) of observing the effect size(s), if the null
192 hypothesis of zero difference is true. For each permutation p value, 5000 reshuffles of the control and test
193 labels were performed; $p < 0.05$ is considered a significant difference. Pearson correlation was applied to
194 calculate the correlation between pain sensitivity and electrophysiological data. The significance threshold
195 for all correlation tests was set at $p < 0.05$.

196 **Results**

197 **Early life pain (ELP) increases injury induced hyperalgesia and pain in adult life**

198 Behavioural pain threshold testing confirmed the impact of early life pain upon adult pain behaviour, as
199 described previously (Beggs et al., 2012; Moriarty et al., 2019). We measured the amplitude and duration of
200 hindlimb withdrawal reflexes in response to electronic von Frey hair stimulation following incision injury in
201 adult male rats. Figure 1 shows von Frey hair pain thresholds in adult ELP male rats before and 10 days after
202 an adult hindpaw incision (II). This is compared to age- matched animals with no ELP, experiencing their first
203 hindpaw incision in adulthood (NI) and control rats that have ELP only or no incisions at all (Con) (Figure 1).

204 Hindpaw incision injury caused von Frey hair thresholds to fall in both groups of adult rats (NI and II)
205 compared to the control (Con) group, indicating a significant post injury pain and hyperalgesia. Consistent
206 with previous reports (Beggs et al., 2012b; Moriarty et al., 2019), animals that experienced early life pain
207 (ELP) (II, n=9) developed significantly lower paw withdraw thresholds (PWT), compared to injured animals
208 with no ELP (NI, n=10). In addition, as in earlier studies (Walker et al., 2009b), ELP resulted in more
209 prolonged as well as enhanced hyperalgesia, lasting up to 10 days after hindpaw incision, compared to 3-4
210 days in non ELP rats.

211 **Early life pain (ELP) increases post injury evoked delta and gamma activity in adult S1**

212 To test the impact of early life pain experience upon pain related neural activity in S1 and mPFC, we next
213 investigated evoked potentials (EP) and oscillatory neural activity in S1 and mPFC evoked by mechanical
214 stimulation (von Frey hair, eVF) following incision injury. Evoked potential (EP) amplitudes in S1 and mPFC
215 did not differ between groups and so to gain further insight into the pattern and time-course of evoked
216 cortical activity following incision injury, the EP energy was analysed in the delta (2–4 Hz), theta (4–8 Hz),
217 alpha (8–12 Hz), beta (12–30 Hz), and gamma (30–90 Hz) frequency bands. Fig 3 & Fig 4 show a significant
218 increase in the eVF evoked delta energy (Fig 3C,D) and gamma energy (Fig 4C,D) in S1 following incision in
219 ELP rats, which is not observed in the other adult rat groups, NI and Con. The sensory evoked data in Figs 3
220 and 4 has been normalized to baseline (a period before stimulation), removing any effect of increased
221 gamma power in the S1 and PFC caused by the surgical pain alone, and revealing only eVF stimulus evoked
222 energy changes. These stimulus evoked increases in delta and gamma energy in ELP rats were recorded in II
223 groups only, in the 2-3 hours post injury (D0) and had recovered by 4 days post injury. They were not
224 observed in mPFC

225 Importantly, the magnitude of S1 evoked delta and gamma activity was significantly correlated to pain
226 sensitivity, or fall in behavioural von Frey hair paw withdrawal threshold (PWT), as indicated by the inverse
227 correlation of S1 delta power (Fig 3E) and S1 gamma power (Fig 4E) with PWT in II male adult rats.

228 **Early life pain (ELP) increases post injury evoked delta-gamma coupling in adult S1**

229 Since delta and gamma energy evoked by mechanical stimulation (eVF) post injury is increased in S1 in ELP
230 rats, we next asked whether ELP altered cross-frequency coupling (delta (2-4Hz) vs. gamma (30-90 Hz))
231 associated with the observed differences in pain sensitivity following hindpaw incision. Cross-frequency
232 interaction (Florin and Baillet, 2015). Here, in order to evaluate event related changes in phase-amplitude
233 coupling, we used time-resolved phase-amplitude coupling (tPAC). Fig 5 shows a significant enhancement of
234 evoked delta-gamma coupling in S1 immediately post-incision (D0) in II rats (Figure 5 A-C). This increase in
235 delta-gamma coupling was not seen in mPFC (Figure 5D). The enhanced evoked delta-gamma coupling in S1
236 coupling potentially provides a mechanism for investigating local-to-wide networks synchronization and was
237 observed on the day of injury and return to pre-injury levels by 4 days (D4) post-incision in II rats. There was
238 no significant alteration in S1 evoked delta-gamma coupling in NI and Con rats (Figure 5E). To determine
239 whether this increase in evoked S1 delta-gamma coupling is associated with the enhanced pain sensitivity,
240 we subsequently examined the correlation between the two measures. A significant inverse correlation was

241 found between delta-gamma coupling and paw withdrawal threshold in II rats, but not in NI and Con rats
242 (Figure 5F). Thus, pain related stimulus evoked delta-gamma coupling in the somatosensory cortex and its
243 association with pain behaviours is selectively increased in adult ELP rats.

244 **Early life pain (ELP) increases post injury evoked S1-mPFC connectivity in adult rats**

245 The increased pain related signal processing in ELP found in adult S1, was not observed in mPFC. Since
246 alterations in pain processing in mPFC may depend upon connections with other areas of the cerebral
247 cortex, we next examined the functional connectivity between the S1 and mPFC in ELP rats. To explore this,
248 we used phase locking value (PLV), a statistical method used to investigate task-induced changes in long
249 range synchronization of neural activity (Lachaux et al., 1999) which provides an index of phase synchrony
250 between two signals over a specific time period.

251 On the day of injury (D0), 2-3 hours after the incision, a significant increase in S1-mPFC PLV in response to
252 eVF stimulation occurred in both ELP and non ELP rats following hindpaw incision (NI and II). There was no
253 significant difference between the two injured groups (Figure 6 A-C). This increase in phase locking was
254 restricted to the theta band and was not observed in other frequency bands (Delta: $F_{(2, 28)} = 0.16$, $P=0.85$;
255 Alpha: $F_{(2, 28)} = 1.75$, $P=0.19$; Beta: $F_{(2, 28)} = 0.96$, $P=0.39$; Gamma: $F_{(2, 28)} = 2.41$, $P=0.10$). Importantly, a clear
256 difference emerges upon inspection of the time course of this effect post injury, which reveals that the
257 increased theta phase locking is maintained until 4 days post-injury in ELP (II) rats, compared to non-ELP (NI)
258 groups (Figure 6D and 6E). We further examined correlation coefficients with pain behaviour to determine
259 whether the increased S1-mPFC PLV in the theta band is associated with pain hypersensitivity. A significant
260 inverse correlation between S1-mPFC PLV and PWT is seen in both NI and II rats, but not in uninjured Con
261 rats (Figure 6F).

262 **Discussion**

263 The results presented here provide novel insights into the effects of ELP upon adult cortical pain networks.
264 Using telemetric recording of local field potentials in the S1 and mPFC in awake adult mice we show that ELP
265 results in significant changes in neural connectivity in the adult S1 and mPFC related to post-injury pain
266 hypersensitivity.

267 We used a well-established model of ELP, incision on the plantar hindpaw, which when applied at a critical
268 stage of development, is known to cause lasting changes in pain behaviour and increased post-injury pain
269 hypersensitivity in adult life (Walker et al., 2009b; Beggs et al., 2012b; Schwaller and Fitzgerald, 2014). The
270 effect is likely to be driven by altered peripheral nociceptor sensitization (Jankowski et al., 2014; Walker et
271 al., 2016; Dourson et al., 2021) and microglial activation in the dorsal horn of the spinal cord (Beggs et al.,
272 2012b; Moriarty et al., 2019) resulting in altered synaptic connectivity and reduced dynorphin inhibition in
273 the dorsal horn of the spinal cord (Li and Baccei, 2016, 2019; Brewer et al., 2020). Brainstem descending pain
274 control is also altered in adults following early life incision (Walker et al., 2015) but the current data is the
275 first to show changes in functional cortical pain networks following ELP. By recording simultaneous
276 behavioural and cortical LFP responses to the same mechanical stimulus, we show that following ELP delta
277 and gamma energy and delta/gamma modulation are increased in S1, together with increased phase-locking
278 connectivity with mPFC, all directly correlated with behavioural pain hypersensitivity.

279 The data provide new insight into the central mechanisms whereby exposure to painful sensory experience
280 in early life alters adult pain experience. The mPFC and S1 have key roles in cortical pain processing (Tan and
281 Kuner, 2021); mPFC receives ascending nociceptive input, but also exerts important top-down regulation of
282 sensory and affective processes of pain (Kummer et al., 2020), whereas S1 is the first level of pain perception
283 and encodes nociceptive intensity and perceived pain intensity (Fields, 2012; Mancini et al., 2012). Pain is a
284 complex phenomenon that depends on communication between different brain areas, which is served by

285 neural oscillations and connectivity involving short-range and long-range communication processes (Baliki et
286 al., 2011; Baliki and Apkarian, 2015; Kucyi and Davis, 2015; Ploner et al., 2017; Tan et al., 2021) and it is
287 these oscillations that we have focussed on here.

288 The results reveal a significantly greater noxious-evoked gamma in S1 in injured rats with ELP compared to
289 controls. In humans, gamma-band oscillations in the primary somatosensory cortex correlate with subjective
290 pain perception (Zhang et al., 2012; Heid et al., 2020) and in mice they are specifically strengthened,
291 independently of any motor component, in the S1 cortex during nociception and are elevated during pain
292 hypersensitivity (Tan et al., 2019). Nociceptive C fibre stimulation drives gamma activity in adult rat S1
293 (Chang et al., 2020b) and gamma oscillations generated by optogenetic activation of parvalbumin-expressing
294 inhibitory interneurons in the S1 cortex enhance nociceptive sensitivity and induce aversive avoidance
295 behaviour, while activating a network of prefrontal cortical and subcortical centres including descending
296 serotonergic facilitatory pathways (Tan et al., 2021). Recent evidence suggests that gamma oscillations
297 reflect strongly coupling of neural activity with fast spiking interneurons in the superficial layers of the S1
298 contralateral to the stimulated side (Yue et al., 2020a). The increased energy of gamma oscillations,
299 considered one of the most promising biomarkers of pain in the brain, is important evidence for increased
300 post injury pain perception in ELP animals.

301 Evoked activity in the delta frequency was also observed in the S1 of injured ELP rats. Event-related delta
302 oscillations serve active sensory and cognitive functional roles across different sensory domains (Arnal and
303 Giraud, 2012; Knyazev, 2012; Fardo et al., 2017) and play an crucial role in S1 sensory perception (Schroeder
304 and Lakatos, 2009). Delta oscillations association with pain has been demonstrated elsewhere and may
305 reflect coupling in thalamocortical loops (Sarnthein et al., 2006; Walton et al., 2010; Peng and Tang, 2016).
306 The lack of delta frequency changes in mPFC supports the proposal that thalamo-S1 pathways are altered in
307 ELP rats. Indeed, in human infants, ELP is associated with volume loss in the somatosensory thalamus
308 accompanied by disruptions in thalamic metabolic growth and thalamocortical pathway maturation
309 (Brummelte et al., 2012; Duerden et al., 2018).

310 Neural oscillations play an important role in the integration and segregation of brain regions that are
311 important for pain processing. Low-frequency oscillations (e.g., delta, theta) mediate long-range
312 communication at slow timescales across distant brain regions and are crucial for functional integration in
313 large-scale brain networks. In contrast, high-frequency brain oscillations (e.g., gamma) are more transient
314 and focal and thus important for local neuronal synchrony in cortical areas (Canolty and Knight, 2010).
315 Understanding these spatiotemporal and oscillatory aspects in the context of pain-related neural responses
316 will therefore inform the neural mechanisms underlying pain-sensation. Studies of neural oscillations related
317 to pain have identified several functional bands, especially theta, delta, and gamma bands, implicated in
318 nociceptive processing (Kim and Davis, 2021; Luo et al., 2021). Delta oscillations are changes in the thalamus
319 and S1, as well as the coupling between the thalamus and S1, in laser-induced pain (Li et al., 2017) and in
320 neuropathic disease (Walton et al., 2010). Furthermore, a recent study suggested that the delta combined
321 with other oscillations is responsible for the coding of pain perception, indicating that perception as an
322 overall reflection of the pain state may contain complex information and involve additional brain areas (Luo,
323 2021). On the other hand, gamma oscillations in S1 predict the pain intensity induced by laser stimulation in
324 both humans and rodents (Hu and Iannetti, 2019; Yue et al., 2020b) and the pain level in chronic pain
325 patients (Parker et al., 2020), indicating gamma oscillations may contain more specific information about
326 pain. Therefore, the combination of neural oscillations is essential for encoding perceptive and sensory
327 measures of pain. Our findings highlight that pain related sensory evoked neuronal activity in S1 which is
328 associated with both low- and high-frequency oscillatory rhythms, mediating functional integration at both
329 local and large-scale brain networks are altered by early life pain experiences.

330 Overall, these results indicate that the changes in delta and gamma activity in S1 are functionally linked to
331 the behavioural hypersensitivity in injured rats with ELP. However, given the distinct intrinsic spatiotemporal
332 properties of low- and high-frequency oscillations, we further examined the transient modulation of high-
333 frequency amplitude (gamma) by low-frequency phase (delta) in relation to pain sensitivity and found
334 enhanced evoked S1 delta-gamma modulation in injured rats with ELP. Because the high-frequency activity
335 reflects local cortical processing, while low-frequency brain rhythms are dynamically entrained across
336 distributed brain regions by both external sensory input and internal cognitive events, cross frequency
337 modulation between low and high frequency is thought to contribute to information flow from large-scale
338 brain networks to the fast, local cortical processing (Cardin et al., 2009; Canolty and Knight, 2010). Phase-
339 amplitude cross-frequency coupling strength changes quickly in response to sensory, motor, and cognitive
340 events (Schroeder and Lakatos, 2009) and abnormalities of cross frequency modulation may contribute to
341 abnormal routing of information flow in chronic pain (Ploner et al., 2017). Our results suggest that such
342 abnormal routing of information may occur in adults following ELP.

343 While the S1 reflects sensory discriminative aspects of pain, the prefrontal cortex is associated with the
344 affective aspect of pain, providing top-down modulation of sensory and affective processes, including
345 inhibition of both sensory and affective pain signals by descending projections to the various brain and spinal
346 cord regions (Ji and Neugebauer, 2014; Bräscher et al., 2016; Kummer et al., 2020). Enhanced functional
347 connectivity under procedural pain has been observed in several areas involved in pain perception:
348 somatosensory cortices, anterior insula, anterior cingulate cortex and thalamus and mPFC (Bräscher et al.,
349 2016; Galambos et al., 2019). Here we tested whether communication between S1 and mPFC was affected
350 by ELP using synchronisation in the theta range as a measure of connectivity. Theta synchronization is
351 proposed to be involved in large scale integration between long range multiple brain regions (von Stein and
352 Sarnthein, 2000), especially in mPFC (Colgin, 2011; O'Neill et al., 2013; Esmaeili and Diamond, 2019),
353 consistent with human data showing that prefrontal-sensorimotor connectivity is increased in tonic pain
354 (Nickel et al., 2020). Our results show that adult incision injury does indeed produce a marked increase in
355 evoked theta S1–mPFC connectivity, highly correlated to behavioural pain sensitivity in both ELP and control
356 groups, but this increase is prolonged in ELP, lasting for 4 days compared to only one day in controls. Our
357 data suggests that the connection between sensory and affective pain processing is enhanced in ELP rats
358 which may underpin the wider social, emotional and cognitive life-long impact of ELP beyond increased pain
359 perception (Ranger et al., 2018; de Kort et al., 2021; Ririe et al., 2021) .

360 Our demonstration that ELP affects the cortical dynamics and connectivity underlying adult pain perception
361 has important translational implications. Hospitalised infants exposed to ELP as a result of necessary clinical
362 care, despite efforts to control that exposure (Laudiano-Dray et al., 2020; Eccleston et al., 2021), display long
363 term structural and functional brain changes (Ranger and Grunau, 2014; Walker, 2019). Early life adversity,
364 including stress and pain, has been reported to increase the risk of persistent pain in adults (Victoria and
365 Murphy, 2016, 2016; Nelson et al., 2017) and it is possible that the changes reported here underlie an
366 increased vulnerability to chronic pain in adults exposed to ELP. Pain is the perceptual consequence of the
367 complex interactions of many cortical areas, including the somatosensory, prefrontal cortices, and limbic
368 areas (e.g., thalamus) and both animal (Eto et al., 2011) and human (Geha et al., 2008; Ichesco et al., 2012)
369 studies reveal functional and structural changes in these specific areas of the cerebral cortex in chronic pain
370 conditions. Furthermore, S1 and mPFC closely interact in chronic pain (Kong et al., 2013; Jones and Sheets,
371 2020; Kummer et al., 2020). This reorganization of local cortical circuits provides a mechanism for abnormal
372 activity underlying chronic pain and early life adversity, including stress and pain, may not only have long-
373 term effects on nociceptive processing, but also increase the risk of persistent pain in the adult by altering
374 normal brain development and function (Brummelte et al., 2012; Schneider et al., 2018; Chau et al., 2019).

375 In conclusion, we have demonstrated that painful sensory experiences in early life have a significant effect
376 on the function of adult pain-related cortical circuits. This change is likely driven by altered peripheral
377 nociceptor and spinal cord circuit function following early life injury. Changes in regional and interregional
378 neural oscillations in S1 and mPFC caused by painful experience in early life play a key role in altered
379 nociceptive processing and may predispose an adaptive mechanism during chronification of pain.
380 Understanding the effects of ELP upon developing cortical pain networks will increase our understanding of
381 individual susceptibility to pain in adult life (Denk et al., 2014).

382 **Acknowledgements**

383 Supported by grants from the Biotechnology and Biological Sciences Research Council (MF, PC)
384 (BB/R00823X/1) and the Medical Research Council (LF, MF) (MR/L019248/1).

385 **Author contributions**

386 MF and PC conceived the study, PC collected the behavioural and electrophysiology data; PC and LF analysed
387 the data; all authors interpreted the data and contributed to the manuscript.

388

389 **References**

390

- 391 Apkarian AV, Bushnell MC, Treede R-D, Zubieta J-K (2005) Human brain mechanisms of pain perception and
392 regulation in health and disease. *European Journal of Pain* 9:463–463.
- 393 Arnal LH, Giraud A-L (2012) Cortical oscillations and sensory predictions. *Trends in Cognitive Sciences*
394 16:390–398.
- 395 Baliki MN, Apkarian AV (2015) Nociception, Pain, Negative Moods, and Behavior Selection. *Neuron* 87:474–
396 491.
- 397 Baliki MN, Baria AT, Apkarian AV (2011) The cortical rhythms of chronic back pain. *J Neurosci* 31:13981–
398 13990.
- 399 Beggs S, Alvares D, Moss A, Currie G, Middleton J, Salter MW, Fitzgerald M (2012a) A role for NT-3 in the
400 hyperinnervation of neonatally wounded skin. *Pain* 153:2133–2139.
- 401 Beggs S, Currie G, Salter MW, Fitzgerald M, Walker SM (2012b) Priming of adult pain responses by neonatal
402 pain experience: maintenance by central neuroimmune activity. *Brain* 135:404–417.
- 403 Boada MD, Gutierrez S, Giffear K, Eisenach JC, Ririe DG (2012) Skin incision-induced receptive field responses
404 of mechanosensitive peripheral neurons are developmentally regulated in the rat. *J Neurophysiol*
405 108:1122–1129.
- 406 Bräscher A-K, Becker S, Hoespli M-E, Schweinhardt P (2016) Different Brain Circuitries Mediating
407 Controllable and Uncontrollable Pain. *J Neurosci* 36:5013.
- 408 Brennan TJ, Vandermeulen EP, Gebhart GF (1996) Characterization of a rat model of incisional pain. *Pain*
409 64:493–502.
- 410 Brewer CL, Li J, O’Conor K, Serafin EK, Baccei ML (2020) Neonatal Injury Evokes Persistent Deficits in
411 Dynorphin Inhibitory Circuits within the Adult Mouse Superficial Dorsal Horn. *J Neurosci* 40:3882–
412 3895.

- 413 Brummelte S, Grunau RE, Chau V, Poskitt KJ, Brant R, Vinall J, Gover A, Synnes AR, Miller SP (2012)
414 Procedural pain and brain development in premature newborns. *Annals of Neurology* 71:385–396.
- 415 Bruns A (2004) Fourier-, Hilbert- and wavelet-based signal analysis: are they really different approaches?
416 *Journal of Neuroscience Methods* 137:321–332.
- 417 Buzsaki G (2004) Neuronal Oscillations in Cortical Networks. *Science* 304:1926–1929.
- 418 Canolty RT, Knight RT (2010) The functional role of cross-frequency coupling. *Trends Cogn Sci* 14:506–515.
- 419 Cao W, Lin S, Xia Q, Du Y, Yang Q, Zhang M, Lu Y, Xu J, Duan S, Xia J, Feng G, Xu J, Luo J (2018) Gamma
420 Oscillation Dysfunction in mPFC Leads to Social Deficits in Neuroigin 3 R451C Knockin Mice. *Neuron*
421 97:1253-1260.e7.
- 422 Cardin JA, Carlén M, Meletis K, Knoblich U, Zhang F, Deisseroth K, Tsai L-H, Moore CI (2009) Driving fast-
423 spiking cells induces gamma rhythm and controls sensory responses. *Nature* 459:663–667.
- 424 Chang P, Bush D, Schorge S, Good M, Canonica T, Shing N, Noy S, Wiseman FK, Burgess N, Tybulewicz VLJ,
425 Walker MC, Fisher EMC (2020a) Altered Hippocampal-Prefrontal Neural Dynamics in Mouse Models
426 of Down Syndrome. *Cell Reports* 30:1152-1163.e4.
- 427 Chang P, Fabrizi L, Fitzgerald M (2020b) Distinct Age-Dependent C Fiber-Driven Oscillatory Activity in the Rat
428 Somatosensory Cortex. *eNeuro* 7:ENEURO.0036-20.2020.
- 429 Chang P, Fabrizi L, Olhede S, Fitzgerald M (2016) The Development of Nociceptive Network Activity in the
430 Somatosensory Cortex of Freely Moving Rat Pups. *Cerebral Cortex* 26:4513–4523.
- 431 Chang P, Hashemi KS, Walker MC (2011) A novel telemetry system for recording EEG in small animals.
432 *Journal of Neuroscience Methods* 201:106–115.
- 433 Chau CMY, Ranger M, Bichin M, Park MTM, Amaral RSC, Chakravarty M, Poskitt K, Synnes AR, Miller SP,
434 Grunau RE (2019) Hippocampus, Amygdala, and Thalamus Volumes in Very Preterm Children at 8
435 Years: Neonatal Pain and Genetic Variation. *Front Behav Neurosci* 13:51.
- 436 Colgin LL (2011) Oscillations and hippocampal–prefrontal synchrony. *Current Opinion in Neurobiology*
437 21:467–474.
- 438 de Kort AR, Joosten EA, Patijn J, Tibboel D, van den Hoogen NJ (2021) Neonatal procedural pain affects state,
439 but not trait anxiety behavior in adult rats. *Dev Psychobiol* 63:e22210.
- 440 De Lima J, Alvares D, Hatch DJ, Fitzgerald M (1999) Sensory hyperinnervation after neonatal skin wounding:
441 effect of bupivacaine sciatic nerve block. *BJA: British Journal of Anaesthesia* 83:662–664.
- 442 Denk F, McMahon SB, Tracey I (2014) Pain vulnerability: a neurobiological perspective. *Nat Neurosci* 17:192–
443 200.
- 444 Dourson AJ, Ford ZK, Green KJ, McCrossan CE, Hofmann MC, Hudgins RC, Jankowski MP (2021) Early Life
445 Nociception is Influenced by Peripheral Growth Hormone Signaling. *J Neurosci* 41:4410–4427.
- 446 Duerden EG, Albanese M-C (2013) Localization of pain-related brain activation: A meta-analysis of
447 neuroimaging data. *Human Brain Mapping* 34:109–149.
- 448 Duerden EG, Grunau RE, Guo T, Foong J, Pearson A, Au-Young S, Lavoie R, Chakravarty MM, Chau V, Synnes
449 A, Miller SP (2018) Early Procedural Pain Is Associated with Regionally-Specific Alterations in
450 Thalamic Development in Preterm Neonates. *J Neurosci* 38:878–886.

- 451 Eccleston C et al. (2021) Delivering transformative action in paediatric pain: a Lancet Child & Adolescent
452 Health Commission. *Lancet Child Adolesc Health* 5:47–87.
- 453 Esmaeili V, Diamond ME (2019) Neuronal Correlates of Tactile Working Memory in Prefrontal and Vibrissal
454 Somatosensory Cortex. *Cell Reports* 27:3167-3181.e5.
- 455 Eto K, Wake H, Watanabe M, Ishibashi H, Noda M, Yanagawa Y, Nabekura J (2011) Inter-regional
456 Contribution of Enhanced Activity of the Primary Somatosensory Cortex to the Anterior Cingulate
457 Cortex Accelerates Chronic Pain Behavior. *J Neurosci* 31:7631.
- 458 Euston DR, Gruber AJ, McNaughton BL (2012) The role of medial prefrontal cortex in memory and decision
459 making. *Neuron* 76:1057–1070.
- 460 Fardo F, Vinding MC, Allen M, Jensen TS, Finnerup NB (2017) Delta and gamma oscillations in operculo-
461 insular cortex underlie innocuous cold thermosensation. *J Neurophysiol* 117:1959–1968.
- 462 Ferrier J, Bayet-Robert M, Dalmann R, El Guerrab A, Aissouni Y, Graveron-Demilly D, Chalus M, Pinguet J,
463 Eschalièr A, Richard D, Daulhac L, Marchand F, Balayssac D (2015) Cholinergic Neurotransmission in
464 the Posterior Insular Cortex Is Altered in Preclinical Models of Neuropathic Pain: Key Role of
465 Muscarinic M2 Receptors in Donepezil-Induced Antinociception. *J Neurosci* 35:16418.
- 466 Ferrier J, Marchand F, Balayssac D (2016) Assessment of Mechanical Allodynia in Rats Using the Electronic
467 Von Frey Test. *Bio-protocol* 6:e1933.
- 468 Fields HL (2012) Pain and the primary somatosensory cortex. *PAIN* 153:742–743.
- 469 Florin E, Baillet S (2015) The brain's resting-state activity is shaped by synchronized cross-frequency coupling
470 of neural oscillations. *Neuroimage* 111:26–35.
- 471 Galambos A, Szabó E, Nagy Z, Édes AE, Kocsel N, Juhász G, Kökönyei G (2019) A systematic review of
472 structural and functional MRI studies on pain catastrophizing. *J Pain Res* 12:1155–1178.
- 473 Geha PY, Baliki MN, Harden RN, Bauer WR, Parrish TB, Apkarian AV (2008) The Brain in Chronic CRPS Pain:
474 Abnormal Gray-White Matter Interactions in Emotional and Autonomic Regions. *Neuron* 60:570–
475 581.
- 476 Heid C, Mouraux A, Treede R-D, Schuh-Hofer S, Rupp A, Baumgärtner U (2020) Early gamma-oscillations as
477 correlate of localized nociceptive processing in primary sensorimotor cortex. *Journal of*
478 *Neurophysiology* 123:1711–1726.
- 479 Ho J, Tumkaya T, Aryal S, Choi H, Claridge-Chang A (2019) Moving beyond P values: data analysis with
480 estimation graphics. *Nature Methods* 16:565–566.
- 481 Hu L, Iannetti GD (2019) Neural indicators of perceptual variability of pain across species. *Proc Natl Acad Sci*
482 *USA* 116:1782.
- 483 Huang W-C, Zucca A, Levy J, Page DT (2020) Social Behavior Is Modulated by Valence-Encoding mPFC-
484 Amygdala Sub-circuitry. *Cell Reports* 32:107899.
- 485 Ichesco E, Quintero A, Clauw DJ, Peltier S, Sundgren PM, Gerstner GE, Schmidt-Wilcke T (2012) Altered
486 Functional Connectivity Between the Insula and the Cingulate Cortex in Patients With
487 Temporomandibular Disorder: A Pilot Study. *Headache: The Journal of Head and Face Pain* 52:441–
488 454.

- 489 Jankowski MP, Ross JL, Weber JD, Lee FB, Shank AT, Hudgins RC (2014) Age-dependent sensitization of
490 cutaneous nociceptors during developmental inflammation. *Mol Pain* 10:34.
- 491 Jones AF, Sheets PL (2020) Sex-Specific Disruption of Distinct mPFC Inhibitory Neurons in Spared-Nerve
492 Injury Model of Neuropathic Pain. *Cell Reports* 31:107729.
- 493 Jones GT, Power C, Macfarlane GJ (2009) Adverse events in childhood and chronic widespread pain in adult
494 life: Results from the 1958 British Birth Cohort Study. *Pain* 143:92–96.
- 495 Jones L, Verriotis M, Cooper RJ, Laudiano-Dray MP, Rupawala M, Meek J, Fabrizi L, Fitzgerald M (2022)
496 Widespread nociceptive maps in the human neonatal somatosensory cortex. *Elife* 11:e71655.
- 497 Liu X, Green KJ, Ford ZK, Queme LF, Lu P, Ross JL, Lee FB, Shank AT, Hudgins RC, Jankowski MP (2017) Growth
498 hormone regulates the sensitization of developing peripheral nociceptors during cutaneous
499 inflammation. *Pain* 158:333–346.
- 500 Ji G, Neugebauer V (2014) CB1 augments mGluR5 function in medial prefrontal cortical neurons to inhibit
501 amygdala hyperactivity in an arthritis pain model. *Eur J Neurosci* 39:455–466.
- 502 Kim JA, Davis KD (2021) Neural Oscillations: Understanding a Neural Code of Pain. *Neuroscientist* 27:544–
503 570.
- 504 Knyazev GG (2012) EEG delta oscillations as a correlate of basic homeostatic and motivational processes.
505 *Neuroscience & Biobehavioral Reviews* 36:677–695.
- 506 Kong J, Spaeth B, Wey H-Y, Cheetham A, Cook AH, Jensen K, Tan Y, Liu H, Wang D, Loggia ML, Napadow V,
507 Smoller JW, Wasan AD, Gollub RL (2013) S1 is Associated with Chronic Low Back Pain: A Functional
508 and Structural MRI Study. *Mol Pain* 9:1744-8069-9–43.
- 509 Kramer MA, Tort ABL, Kopell NJ (2008) Sharp edge artifacts and spurious coupling in EEG frequency
510 comodulation measures. *Journal of Neuroscience Methods* 170:352–357.
- 511 Kucyi A, Davis KD (2015) The dynamic pain connectome. *Trends Neurosci* 38:86–95.
- 512 Kummer KK, Mitrić M, Kalpachidou T, Kress M (2020) The Medial Prefrontal Cortex as a Central Hub for
513 Mental Comorbidities Associated with Chronic Pain. *Int J Mol Sci* 21:3440.
- 514 Lachaux J-P, Rodriguez E, Martinerie J, Varela FJ (1999) Measuring phase synchrony in brain signals. *Human*
515 *Brain Mapping* 8:194–208.
- 516 Laudiano-Dray MP, Pillai Riddell R, Jones L, Iyer R, Whitehead K, Fitzgerald M, Fabrizi L, Meek J (2020)
517 Quantification of neonatal procedural pain severity: a platform for estimating total pain burden in
518 individual infants. *Pain* 161:1270–1277.
- 519 Le Van Quyen M, Foucher J, Lachaux J-P, Rodriguez E, Lutz A, Martinerie J, Varela FJ (2001) Comparison of
520 Hilbert transform and wavelet methods for the analysis of neuronal synchrony. *Journal of*
521 *Neuroscience Methods* 111:83–98.
- 522 Li J, Baccei ML (2016) Neonatal Tissue Damage Promotes Spike Timing-Dependent Synaptic Long-Term
523 Potentiation in Adult Spinal Projection Neurons. *J Neurosci* 36:5405–5416.
- 524 Li J, Baccei ML (2019) Neonatal Injury Alters Sensory Input and Synaptic Plasticity in GABAergic Interneurons
525 of the Adult Mouse Dorsal Horn. *J Neurosci* 39:7815.

- 526 Li X, Zhao Z, Ma J, Cui S, Yi M, Guo H, Wan Y (2017) Extracting Neural Oscillation Signatures of Laser-Induced
527 Nociception in Pain-Related Regions in Rats. *Front Neural Circuits* 11:71.
- 528 Luo H, Huang Y, Green AL, Aziz TZ, Xiao X, Wang S (2021) Neurophysiological characteristics in the
529 periventricular/periaqueductal gray correlate with pain perception, sensation, and affect in
530 neuropathic pain patients. *NeuroImage: Clinical* 32:102876.
- 531 Mancini F, Haggard P, Iannetti GD, Longo MR, Sereno MI (2012) Fine-grained nociceptive maps in primary
532 somatosensory cortex. *J Neurosci* 32:17155–17162.
- 533 Melchior M, Kuhn P, Poisbeau P (2022) The burden of early life stress on the nociceptive system
534 development and pain responses. *European Journal of Neuroscience* 55:2216–2241.
- 535 Moriarty O, Tu Y, Sengar AS, Salter MW, Beggs S, Walker SM (2019) Priming of adult incision response by
536 early life injury: neonatal microglial inhibition has persistent but sexually dimorphic effects in adult
537 rats. *J Neurosci*:1786–18.
- 538 Nelson SM, Cunningham NR, Kashikar-Zuck S (2017) A Conceptual Framework for Understanding the Role of
539 Adverse Childhood Experiences in Pediatric Chronic Pain. *Clin J Pain* 33:264–270.
- 540 Nickel MM, Ta Dinh S, May ES, Tiemann L, Hohn VD, Gross J, Ploner M (2020) Neural oscillations and
541 connectivity characterizing the state of tonic experimental pain in humans. *Human Brain Mapping*
542 41:17–29.
- 543 O’Neill P-K, Gordon JA, Sigurdsson T (2013) Theta Oscillations in the Medial Prefrontal Cortex Are Modulated
544 by Spatial Working Memory and Synchronize with the Hippocampus through Its Ventral Subregion.
545 *The Journal of Neuroscience* 33:14211–14224.
- 546 Ong W-Y, Stohler CS, Herr DR (2019) Role of the Prefrontal Cortex in Pain Processing. *Mol Neurobiol*
547 56:1137–1166.
- 548 Parker T, Huang Y, Raghu ALB, FitzGerald JJ, Green AL, Aziz TZ (2020) Dorsal Root Ganglion Stimulation
549 Modulates Cortical Gamma Activity in the Cognitive Dimension of Chronic Pain. *Brain Sciences* 10:95.
- 550 Paxinos G, Ashwell KWS, Tork I (2013) Atlas of the Developing Rat Nervous System. Academic Press.
- 551 Peng W, Tang D (2016) Pain Related Cortical Oscillations: Methodological Advances and Potential
552 Applications. *Frontiers in Computational Neuroscience* 10:9.
- 553 Ploner M, Sorg C, Gross J (2017) Brain Rhythms of Pain. *Trends Cogn Sci* 21:100–110.
- 554 Ranger M, Grunau RE (2014) Early repetitive pain in preterm infants in relation to the developing brain. *Pain*
555 *Manag* 4:57–67.
- 556 Ranger M, Tremblay S, Chau CMY, Holsti L, Grunau RE, Goldowitz D (2018) Adverse Behavioral Changes in
557 Adult Mice Following Neonatal Repeated Exposure to Pain and Sucrose. *Front Psychol* 9:2394.
- 558 Reynolds ML, Fitzgerald M (1995) Long-term sensory hyperinnervation following neonatal skin wounds.
559 *Journal of Comparative Neurology* 358:487–498.
- 560 Ririe DG, Eisenach JC, Martin TJ (2021) A Painful Beginning: Early Life Surgery Produces Long-Term Behavioral
561 Disruption in the Rat. *Front Behav Neurosci* 15:630889.
- 562 Samiee S, Baillet S (2017) Time-resolved phase-amplitude coupling in neural oscillations. *NeuroImage*
563 159:270–279.

- 564 Sarnthein J, Stern J, Aufenberg C, Rousson V, Jeanmonod D (2006) Increased EEG power and slowed
565 dominant frequency in patients with neurogenic pain. *Brain* 129:55–64.
- 566 Schneider J, Duerden EG, Guo T, Ng K, Hagmann P, Bickle Graz M, Grunau RE, Chakravarty MM, Hüppi PS,
567 Truttman AC, Miller SP (2018) Procedural pain and oral glucose in preterm neonates: brain
568 development and sex-specific effects. *PAIN* 159:515–525.
- 569 Schroeder CE, Lakatos P (2009) Low-frequency neuronal oscillations as instruments of sensory selection.
570 *Trends Neurosci* 32:9–18.
- 571 Schwaller F, Fitzgerald M (2014) The consequences of pain in early life: injury-induced plasticity in
572 developing pain pathways. *Eur J Neurosci* 39:344–352.
- 573 Tadel F, Baillet S, Mosher JC, Pantazis D, Leahy RM (2011) Brainstorm: A User-Friendly Application for
574 MEG/EEG Analysis Oostenveld R, ed. *Computational Intelligence and Neuroscience 2011*:879716.
- 575 Tan LL, Kuner R (2021) Neocortical circuits in pain and pain relief. *Nat Rev Neurosci* 22:458–471.
- 576 Tan LL, Oswald MJ, Heinl C, Retana Romero OA, Kaushalya SK, Monyer H, Kuner R (2019) Gamma oscillations
577 in somatosensory cortex recruit prefrontal and descending serotonergic pathways in aversion and
578 nociception. *Nature Communications* 10:983.
- 579 Tan LL, Oswald MJ, Kuner R (2021) Neurobiology of brain oscillations in acute and chronic pain. *Trends*
580 *Neurosci* 44:629–642.
- 581 Torsney C, Fitzgerald M (2003) Spinal dorsal horn cell receptive field size is increased in adult rats following
582 neonatal hindpaw skin injury. *J Physiol (Lond)* 550:255–261.
- 583 van den Hoogen NJ, Patijn J, Tibboel D, Joosten BA, Fitzgerald M, Kwok CHT (2018) Repeated touch and
584 needle-prick stimulation in the neonatal period increases the baseline mechanical sensitivity and
585 postinjury hypersensitivity of adult spinal sensory neurons. *Pain* 159:1166–1175.
- 586 Victoria NC, Murphy AZ (2016) Exposure to Early Life Pain: Long Term Consequences and Contributing
587 Mechanisms. *Curr Opin Behav Sci* 7:61–68.
- 588 von Stein A, Sarnthein J (2000) Different frequencies for different scales of cortical integration: from local
589 gamma to long range alpha/theta synchronization. *International Journal of Psychophysiology*
590 38:301–313.
- 591 Walker SM (2019) Long-term effects of neonatal pain. *Semin Fetal Neonatal Med* 24:101005.
- 592 Walker SM, Beggs S, Baccei ML (2016) Persistent changes in peripheral and spinal nociceptive processing
593 after early tissue injury. *Experimental Neurology* 275:253–260.
- 594 Walker SM, Fitzgerald M, Hathway GJ (2015) Surgical injury in the neonatal rat alters the adult pattern of
595 descending modulation from the rostroventral medulla. *Anesthesiology* 122:1391–1400.
- 596 Walker SM, Franck LS, Fitzgerald M, Myles J, Stocks J, Marlow N (2009a) Long-term impact of neonatal
597 intensive care and surgery on somatosensory perception in children born extremely preterm. *Pain*
598 141:79–87.
- 599 Walker SM, O'Reilly H, Beckmann J, Marlow N, EPICure@19 Study Group (2018) Conditioned pain
600 modulation identifies altered sensitivity in extremely preterm young adult males and females. *Br J*
601 *Anaesth* 121:636–646.

- 602 Walker SM, Tochiki KK, Fitzgerald M (2009b) Hindpaw incision in early life increases the hyperalgesic
 603 response to repeat surgical injury: critical period and dependence on initial afferent activity. *Pain*
 604 147:99–106.
- 605 Walton KD, Dubois M, Llinás RR (2010) Abnormal thalamocortical activity in patients with Complex Regional
 606 Pain Syndrome (CRPS) Type I. *PAIN* 150:41–51.
- 607 Yue L, Iannetti GD, Hu L (2020a) The Neural Origin of Nociceptive-Induced Gamma-Band Oscillations. *J*
 608 *Neurosci* 40:3478–3490.
- 609 Yue L, Iannetti GD, Hu L (2020b) The Neural Origin of Nociceptive-Induced Gamma-Band Oscillations. *J*
 610 *Neurosci* 40:3478.
- 611 Zhang Z, Gadotti VM, Chen L, Souza IA, Stenkowski PL, Zamponi GW (2015) Role of Prelimbic GABAergic
 612 Circuits in Sensory and Emotional Aspects of Neuropathic Pain. *Cell Reports* 12:752–759.
- 613 Zhang ZG, Hu L, Hung YS, Mouraux A, Iannetti GD (2012) Gamma-band oscillations in the primary
 614 somatosensory cortex—a direct and obligatory correlate of subjective pain intensity. *J Neurosci*
 615 32:7429–7438.

616

617 **Figure Legends**

618 **Figure 1. Experiment design** (A) Schematic of experimental groups. II: neonatal incision on postnatal day 3
 619 and repeat incision 2 months later in adulthood (ELP model). NI: littermate control with equivalent
 620 anaesthesia, handling and maternal separation on post-natal day 3 and first incision in adulthood. Con:
 621 pooled data from animals having neonatal incision only and from age-matched non-incised litter mates from
 622 the same colony. (B) Experimental protocol for probing the impact of early life pain (ELP) on adult cortical
 623 pain processing and pain behaviour. Upper scale: timeline for recording cortical local field potentials (LFP)
 624 and pain behaviour, where * marks days of simultaneous electronic von Frey hair (eVF) stimulation and LFP
 625 recording. Lower box: Detail of testing protocol for recording resting LFPs and eVF evoked LFP recording. (C)
 626 Schematic of the experimental set-up for simultaneous recording of neural LFP activity in medial prefrontal
 627 cortex (mPFC) and primary somatosensory cortex (S1) in awake adult rats using wireless telemetry while
 628 applying electronic von Frey hairs (eVF) to the plantar hindpaw. (D) Sample traces of simultaneous S1 and
 629 mPFC evoked potentials evoked by mechanical eVF stimulation of the plantar hindpaw.

630 **Figure 2: Early life pain (ELP) increases hyperalgesia following incision injury in adult rats.** (A) Electronic
 631 von Frey hair (eVF) testing of the plantar hindpaw adjacent to the wound (B) Plot of contralateral mechanical
 632 paw withdrawal thresholds (PWT), before (Pre) and up to 10 days (D) after hindpaw incision in adult rats.
 633 Mean \pm SEM with individual data superimposed. (B) Statistical differences between groups using generalized
 634 linear models (C) Summary the post-hoc pairwise comparisons with Bonferroni correction. * $P < 0.05$,
 635 ** $P < 0.01$ *** $p < 0.001$. Non-incised controls (Con, $n=18$), incision in adults without neonatal incision (NI,
 636 $n=10$) and incision in adults with neonatal incision (II, $n=9$).

637 **Figure 3: Stimulus-evoked delta energy in S1 increases after adult incision injury only in animals who**
 638 **experienced early life pain.** Electrophysiological responses in the (A) somatosensory cortex (S1) and (F)
 639 medial prefrontal cortex (mPFC) to mechanical (eVF) stimulation of the hindpaw following adult injury in ELP
 640 rats (II, red) and non-ELP rats (NI, blue) and controls (Con, black). Peristimulus normalised delta frequency
 641 (2-4 Hz) oscillations (mean \pm SEM) in S1 (B) and mPFC (G) on the day of adult incision injury (D0). Comparison
 642 of the injury-induced changes in stimulus-evoked delta energy in S1 (C) and mPFC (H), expressed as a ratio of
 643 normalized magnitude (D0/Pre), between groups. (D) The enhancement of injury-induced changes in sensory

644 evoked S1 delta energy returned to pre-injury level by 10 days (D10) following injury. The paired mean
 645 difference for comparisons is shown as Cumming estimation. Each paired mean difference is plotted as a
 646 bootstrap sampling distribution; 95% confidence intervals are indicated by the ends of the vertical error
 647 bars. Statistical analysis was performed using a permutation t-test (Randomization: 5000). (E) Correlations
 648 between paw withdrawal threshold (PWT) and stimulus-evoked S1 delta activity (normalized magnitude).
 649 The scatter plots represent the correlations between PWT and normalized energy (Pre to D10) with
 650 continuous lines showing the linear regression. Pearson correlation coefficient (R) with significance (P value)
 651 is presented in the figures. Non-incised adult controls (Con, n=15), incision in adults without neonatal
 652 incision (NI, n=8), and incision in adults with neonatal incision (II, n=8).

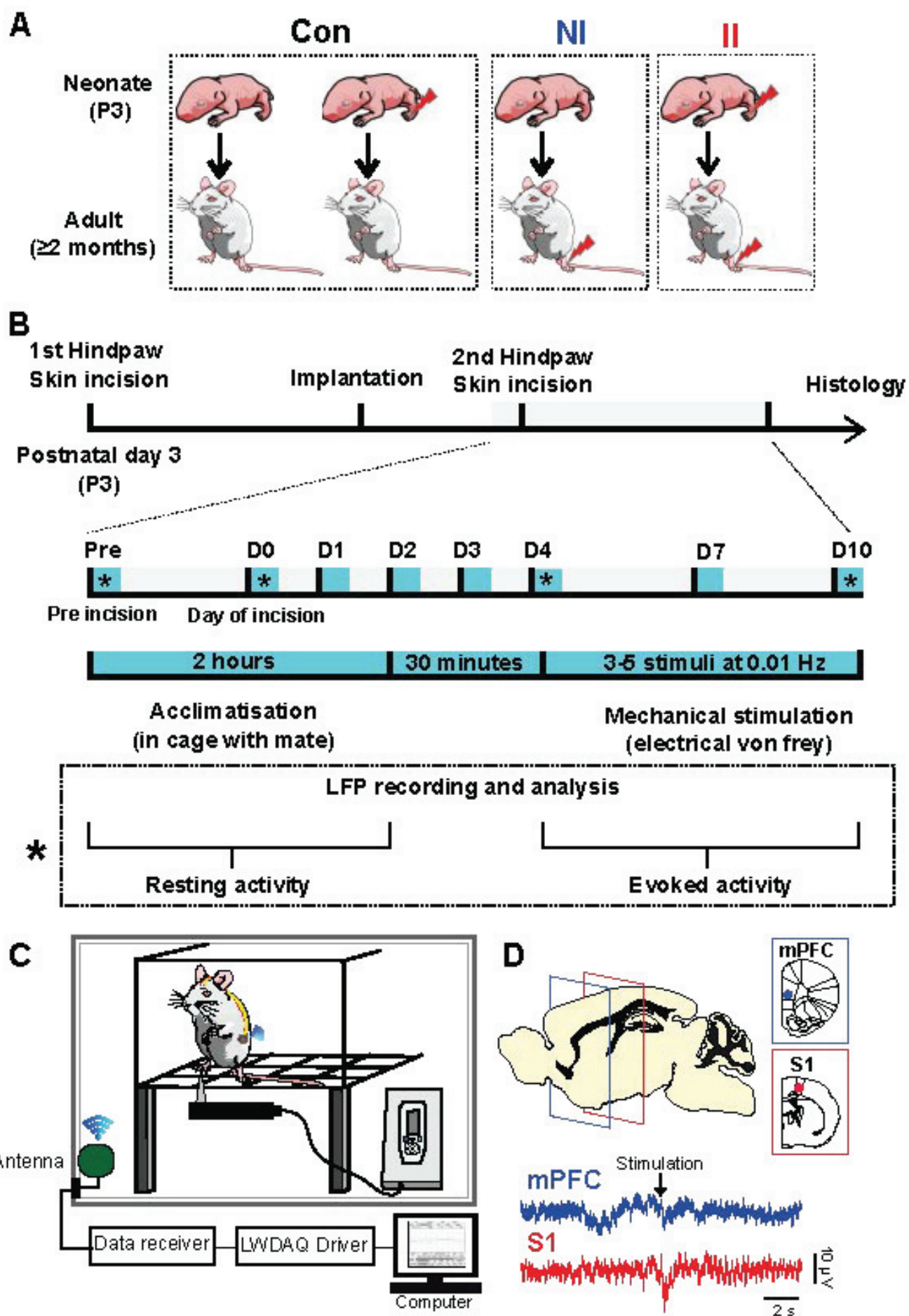
653 **Figure 4: Stimulus-evoked gamma energy in S1 increases after adult incision injury only in animals who**
 654 **experienced early life pain.** Electrophysiological responses in the (A) somatosensory cortex (S1) and (F)
 655 medial prefrontal cortex (mPFC) to mechanical (eVF) stimulation of the hindpaw following injury in ELP adult
 656 rats (II, red), non-ELP rats (NI, blue) and controls (Con, black). Peristimulus normalised gamma frequency (30-
 657 90 Hz) oscillations (mean \pm SEM) in S1 (B) and mPFC (G). Comparison of changes in stimulus-evoked gamma
 658 energy in S1 (C) and mPFC (H), expressed as a ratio of normalized magnitude (D0/Pre), between groups. (D)
 659 The enhancement of injury-induced changes in sensory evoked S1 gamma energy returned to pre-injury
 660 level by 4 days (D4) following injury. The paired mean difference for comparison is shown as Cumming
 661 estimation. Each paired mean difference is plotted as a bootstrap sampling distribution; 95% confidence
 662 intervals are indicated by the ends of the vertical error bars. Statistical analysis was performed using a
 663 permutation t-test (Randomization: 5000). (E) Correlations between paw withdrawal threshold (PWT) and
 664 stimulus evoked S1 gamma activity (normalized magnitude). The scatter plots represent the correlations
 665 between PWT and normalized energy (Pre to D10) with continuous lines showing the linear regression.
 666 Pearson correlation coefficient (R) with significance (P value) is presented in the figures. Non-incised adult
 667 controls (Con, n=15), incision in adults without neonatal incision (NI, n=8), and incision in adults with
 668 neonatal incision (II, n=8).

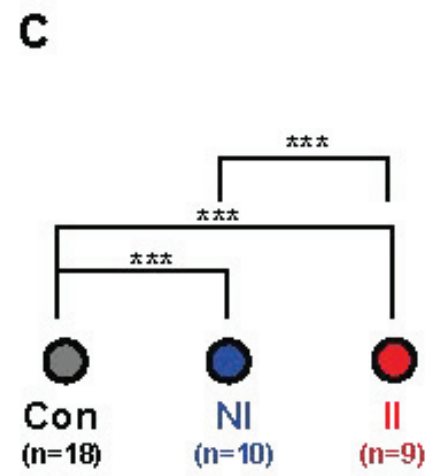
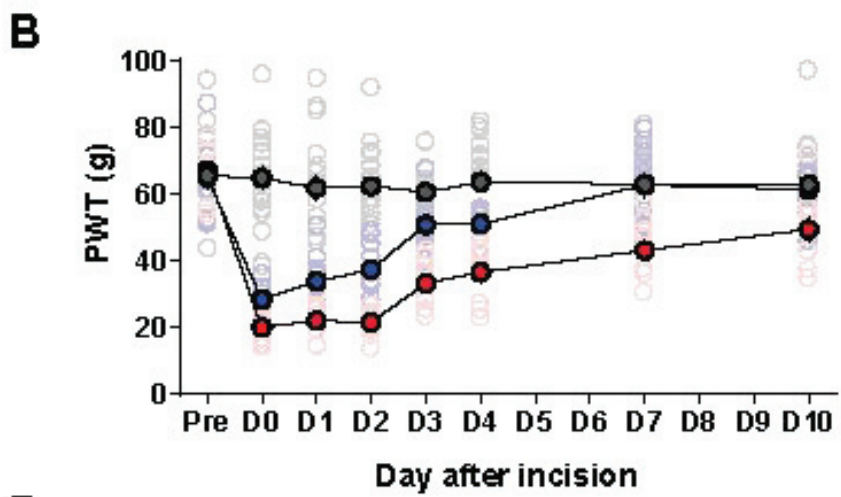
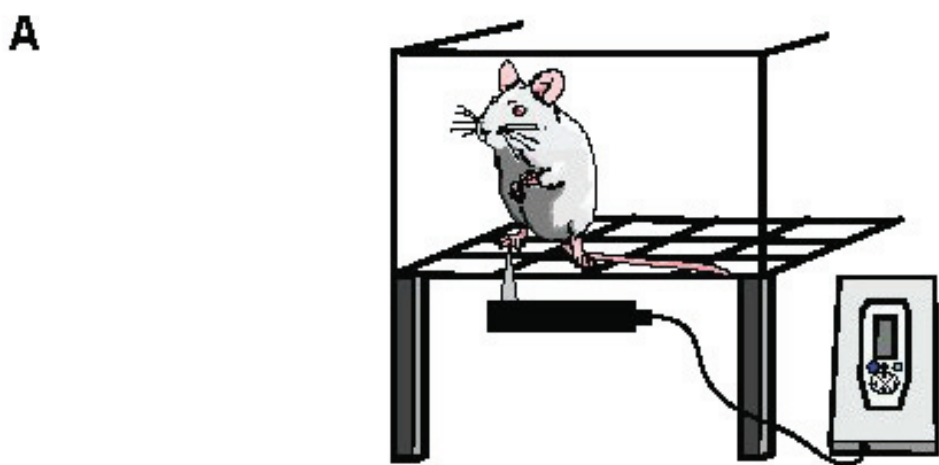
669 **Figure 5. Stimulus-evoked delta-gamma cross-frequency coupling in S1 increases after adult injury only in**
 670 **animals who experienced early life pain.** (A) Sample trace of LFP recorded in S1 during hindpaw mechanical
 671 stimulation (eVF) and a diagram illustrating the principle of cross-frequency coupling. Peristimulus
 672 normalised time-resolved delta-gamma coupling in S1 (B) and mPFC (D) on the day of adult injury (D0), data
 673 are presented as mean \pm SEM. (C) Comparison of the injury-induced changes in stimulus-evoked delta-
 674 gamma coupling in S1, expressed as a ratio of normalized magnitude (D0/Pre), between groups. (E) The
 675 enhancement of pain-induced changes in stimulus-evoked delta-gamma coupling in S1 returned to pre-injury
 676 level by 4 days (D4) following injury. The paired mean difference for comparisons is shown as Cumming
 677 estimation. Each paired mean is plotted as a bootstrap sampling distribution; 95% confidence intervals are
 678 indicated by the ends of the vertical error bars. Statistical analysis was performed using permutation t-test
 679 (Randomization: 5000). (F) Correlations between paw-withdraw threshold (PWT) and delta-gamma
 680 modulation in S1 expressed as normalized modulation index. The scatter plots represent correlations
 681 between PWT and normalized delta-gamma coupling with continuous line as linear regression. Pearson
 682 correlation coefficient (R) with significance (P value) * $p < 0.05$, ** $P < 0.01$. Non-incised adult controls (Con,
 683 n=15), incision in adults without neonatal incision (NI, n=8) and incision in adults with neonatal incision (II,
 684 n=8).

685 **Figure 6: Stimulus-evoked S1-mPFC beta phase coupling is enhanced after adult injury and is prolonged in**
 686 **animals who experienced early life pain** (A) An example of simultaneous recording of stimulus evoked LFPs
 687 in S1 and mPFC, before (left) and after (right) filtering for phase coupling measurement at theta frequency
 688 (B) Peristimulus normalised S1-mPFC phase-locking value (PLV) at theta frequency following injury,
 689 presented as mean \pm SEM. (C) Comparison of changes in S1-mPFC PLV at theta on the day of injury (D0) and

690 (D) 4 days following injury (D, D4), expressed as a ratio of normalized PLV (D0/Pre), between groups. (E) The
691 enhancement of injury induced changes in sensory evoked S1-mPFC PLV at theta returned to pre-injury level
692 by 4 days (D4) in the NI group, whereas a longer lasting increase in S1-mPFC PLV at theta was found in II. as a
693 bootstrap sampling distribution, 95% confidence intervals are indicated by the ends of the vertical error
694 bars. Statistical analysis was performed using a permutation t-test (Randomization: 5000). (F) Correlations
695 between paw-withdraw threshold (PWT) and stimulus evoked S1-mPFC phase lock theta oscillations. The
696 scatter plots represent correlations between PWT and normalized delta-gamma coupling with continuous
697 line as linear regression. Pearson correlation coefficient (R) with significance (P value) * $p < 0.05$, ** $p < 0.01$.
698 Non-incised adult controls (Con, $n=15$), incision in adults without neonatal incision (NI, $n=8$) and incision in
699 adults with neonatal incision (II, $n=8$).

700





D

	Pre	D0	D1	D2	D3	D4	D5	D6	D7	D8	D9	D10
CON vs NI	ns	***	***	***	***	ns			ns			ns
CON vs II	ns	***	***	***	***	***			***			ns
NI vs II	ns	ns	ns	ns	*	ns			**			ns

